Journal of Alloys and Compounds 509 (2011) 6852–6858

Contents lists available at ScienceDirect

Journal of Alloys and Compounds

journal homepage: www.elsevier.com/locate/jallcom

Characterization and dissolution–reprecipitation behavior of biphasic tricalcium phosphate powders

Chao Zou[a,b], Kui Cheng[a], Wenjian Weng[a,*], Chenlu Song[a], Piyi Du[a], Ge Shen[a], Gaorong Han[a]

[a] Department of Materials Science & Engineering, State Key Laboratory of Silicon Materials, Zhejiang University, Hangzhou 310027, PR China
[b] Nanomaterials & Chemistry Key Laboratory, College of Chemistry and Material Engineering, Wenzhou University, Wenzhou 325027, PR China

ARTICLE INFO

Article history:
Received 23 October 2010
Received in revised form 28 March 2011
Accepted 29 March 2011
Available online 5 April 2011

Keywords:
TCP
Biphase
Dissolution
Reprecipitation

ABSTRACT

α-tricalcium phosphate (α-TCP), biphasic α/β-tricalcium phosphate (α/β-TCP) with different two phase ratio and β-tricalcium phosphate (β-TCP) powders were prepared by calcining an amorphous calcium phosphate (ACP) precursor at a temperature ranging from 800 to 900 °C. The microstructural characterization revealed that the particles in the monophasic and the biphasic TCP powders had about 1 μm in size, and agglomerated by 500 nm ones. In comparison with monophasic TCP powders, the dissolution–reprecipitation behaviors of the biphasic TCP powders in an acetate buffer solution with pH 5 were studied. The biphasic TCPs demonstrated a different behavior from the monophasic TCPs, including changes in morphology and crystalline phase. The unique behavior can be tailored by controlling the α-TCP content in the biphasic TCP powders.

1. Introduction

Tricalcium phosphate ($Ca_3(PO_4)_2$, TCP) is reactive in a body fluid, the reaction process and product can make significant contributions to bone repair and regeneration [1–6]. Consequently, TCP is considered to be one of the most accepted biomaterials as synthetic bone graft substitutes and cements [7–14].

The role of TCP in biological systems depends mostly on its dissolution–reprecipitation behavior. However, TCP has two isomeric crystalline structures, α-TCP (high temperature phase) and β-TCP (low temperature phase). The reaction of α-TCP with solutions is mainly a fast hydrolysis (dissolution–reprecipitation) as a phase transformation from α-TCP to brushite or apatite depending on pH value [6]. The reaction process can be used to strengthen the integration of the implant with host tissue and develop suitable microstructures to accommodate bone cells and tissues. The reaction of β-TCP with solutions mainly involves a relatively slow dissolution. The reprecipitation occurrence depends on the surrounding concentrations of Ca and phosphate ions, as well as pH value. The reaction process can be adopted to create osteoconductivity through releasing Ca and P ions in course of bone regeneration [7,8].

Recently, it has been found that biphasic Ca phosphate is a good way to make full use of the advantages from each monophasic Ca phosphate for enhancing performances in applications [15–18]. For example, the biphasic β-TCP/HA has demonstrated to have an optimizing biodegradability and osteoconductivity [19,20], and the biphasic β-TCP/amorphous-CPP (calcium polyphosphate) showed significant improvement of degradation with the addition of CPP [21]. Similarly, the biphasic α/β-TCP can be expected to promote the bone formation through adjusting reaction kinetic and controlled dissolution–reprecipitation behavior, which results in the desired ion release, biodegradability and morphological evolution. Although there were few reports on the cell culture on the biphasic α/β-TCP materials [22], it is of great significance to understand the relations of dissolution–reprecipitation behavior with the two-phase ratio and microstructure of the biphasic TCP powders, which might create favorable microstructure and crystalline phase for the bone growth.

Dissolution–reprecipitation behaviors of Ca phosphates are usually evaluated by measuring the Ca and P ion concentrations with soaking time [23–30]. The reaction behavior with soaking time can be monitored by pH variation, which reveals the changes of the ion concentrations in the solution [31]. Although the pH value in a buffer solution can be maintained if the proton or hydroxyl concentration changes within a certain extent, the pH value is sensitive to the presence of weak acidic anions from buffer reagent or multiacidic anions like phosphates. Several buffer solutions have been used as soaking media to evaluate the dissolution behaviors of Ca phosphates. Among them, acetate buffer solution shows almost no influence on the initial Ca phosphate reprecipitation because of no Ca and phosphate ions, and no strong ligands to coordinate Ca ions in the solution. When the body suffers any kind of lesion or inflammatory process, the pH of the media in the affected area decreases

* Corresponding author. Tel.: +86 571 8795 3787; fax: +86 571 8795 3787.
E-mail address: wengwj@zju.edu.cn (W. Weng).

0925-8388/$ – see front matter © 2011 Elsevier B.V. All rights reserved.
doi:10.1016/j.jallcom.2011.03.158

to about 5.0 [32]. Hence, the dissolution experiment performed at pH 5.0 could simulate the situation, and simultaneously shorten test periods due to an accelerating dissolution reaction.

For preparation of biphasic Ca phosphates, the simplest way is to mechanically mix the two-phase powders [17,33], which might not give a desired distribution homogeneity. An incomplete phase transformation has been adopted to prepare the biphasic β-TCP/HA through calcining Ca deficient apatite at 800–1100 °C [34]. Similarly, biphasic α/β-TCP is supposed to be easily obtained by calcining β-TCP powders, since the phase transformation of β-TCP to α-TCP occurs at 1120–1180 °C [35,36]. However, the high temperature calcination leads to a large particle size, broad particle size distribution, and hard agglomeration [37].

In this work, an amorphous Ca phosphate (ACP) precursor way was adopted to synthesize fine monophasic TCP and biphasic TCP powders. The dissolution–reprecipitation behavior of the TCP powders in acetate buffer solution with pH 5 was monitored through pH value variation in the soaking solution. The difference in the behavior from the monophasic TCP powders was discussed along with the characterizations of the soaked biphasic powders.

2. Experimental details

2.1. Materials

$CaCl_2$ (99%), Na_3PO_4 (99%) and Poly(ethylene glycol) (PEG, M_W = 10,000, 99%) were used as starting materials for the synthesis of ACP. Acetic acid ($C_2H_4O_2$, 99.9%) and sodium acetate ($C_2H_3NaO_2$, 98%) were used to prepare the acetate buffer solution. Ethylene dibromide ($C_2H_4Br_2$, 95%) was used as a medium to evaluate the density of TCP powders through a sedimentation test. All chemicals used in this work were purchased from Aladdin.

2.2. Preparation of monophasic and biphasic TCP

$CaCl_2$ and the PEG were dissolved in deionized water to form 0.100 M PEG–$CaCl_2$ solution with a PEG:$CaCl_2$ weight ratio of 4:1. 0.133 M Na_3PO_4 solution was added dropwise into the PEG–$CaCl_2$ solutions in a Ca/P molar ratio of 1.50, the precipitation reaction occurred at pH 9 with ammonia and 5 °C in a water bath for 30 min. The precipitates were filtrated and washed using 5 °C deionized water to remove Cl^- and Na^+ ions. Finally, the precipitate was freeze–dried for 48 h. The freeze–dried powders were used as precursor powders. The precursor powders could be transformed to monophasic and biphasic TCPs by heat-treating at 800–900 °C range for 3 h without gas-protection.

2.3. pH curve measurement during reaction in acetate buffer solution

An acetate buffer solution with pH 5.0 was prepared through mixing a 0.1 M acetic acid solution and a 0.1 M sodium acetate solution in a volume ratio of 1:2. For a pH variation curve measurement, the acetate buffer solution was put into a jacketed glass vessel inserted in a 37 °C water bath; when the buffer solution reached 37 °C, the TCP powder was put into the buffer solution in a ratio of 0.50 g/50 ml with a moderate magnetic stirring speed of 200 rpm; a pencil-size combination pH electrode (E-201-C, Leici shanghai) was used, the pH value data were acquired and recorded by a computer. The pH monitor was assembled in this lab and had a pH accuracy of ±0.02.

In order to simulate the influence of the phosphate concentration on pH value of the buffer solution, a reference curve of the phosphate concentration in the acetate buffer solution versus the pH value was intentionally made by adding a designed amount of Na_3PO_4 into the acetate buffer solution with pH 5.

2.4. Characterizations

The precursor powders, calcined powders and soaked powders were identified by XRD (RIGAKU, D-MAX, RA, CuKα 2°/min, 0.02 per step). In order to determine the α-TCP content in biphasic TCP, a calibration was made for the relationship between the peak intensity in XRD pattern and the α-TCP content in the powders. For the calibration samples, ACP derived α-TCP and β-TCP powders were mixed in weight percentage [$W_{\alpha\text{-TCP}}/(W_{\alpha\text{-TCP}} + W_{\beta\text{-TCP}})$] of 25%, 50% and 75%, respectively. The strongest diffraction lines (034) intensity at 30.7° ($I_{\alpha\text{-TCP}}$) for α-TCP (JCPSD Card No. 29-0359) and (0210) intensity at 31.0° ($I_{\beta\text{-TCP}}$) for β-TCP (JCPSD Card No. 09-0169), were used as an index related to contents. A curve of $I_{\alpha\text{-TCP}}/(I_{\beta\text{-TCP}} + I_{\alpha\text{-TCP}})$ against $W_{\alpha\text{-TCP}}/(W_{\alpha\text{-TCP}} + W_{\beta\text{-TCP}})$ for the mixtures was established as shown in Fig. 1. The α-TCP content in the biphasic TCP obtained in this work was estimated from the curve.

The ACP powders and biphasic powders were observed under Transmission Electron Microscope (JEOL 1200) for a morphological observation. A selected area electron diffraction (SAED) was done to determine the phases of biphasic agglomerated particles. Morphological variations of the powders after soaking in acetate buffer solution were observed under Field Emission Scanning Electron Microscope SEM (FEI SIRION). A sedimentation test in $C_2H_4Br_2$ (2.96 g cm^{-3}) was designed to evaluate the distribution homogeneity of the two-phase particles in the biphasic TCP powders [38], based on the difference in density between α-TCP (2.86 g cm^{-3}) and β-TCP (3.07 g cm^{-3}). The monophasic and biphasic powders were ultrasonically dispersed in $C_2H_4Br_2$ at 25 °C for 10 min. The float and sedimentation status of the powders were photographed after the powders settled down over 24 h.

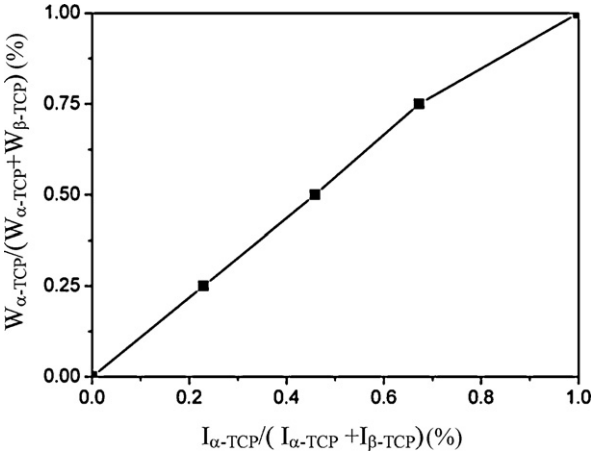

Fig. 1. A relationship of the XRD peak intensity proportion [$I_{\alpha\text{-TCP}}/(I_{\alpha\text{-TCP}} + I_{\beta\text{-TCP}})$] with the phase weight proportion [$W_{\alpha\text{-TCP}}/(W_{\alpha\text{-TCP}} + W_{\beta\text{-TCP}})$].

3. Results

3.1. Characterizations of the powders

The XRD patterns (Fig. 2) show the phase evolution during calcination. The as-freeze–dried precipitates are amorphous. After an 800 °C calcination, the powder crystallizes into pure α-TCP. With increasing the calcination temperature to 830 °C and 850 °C, biphasic α/β-TCP powders are formed. Based on the calibration curve (Fig. 1), 830 °C and 850 °C calcined powders are estimated to contain 60 wt% and 40 wt% α-TCP, respectively. A complete transformation to pure β-TCP occurs when the calcining temperature reaches 900 °C. Obviously, the calcination temperature is a key factor determining the relative phase ratio in final powders. Here,

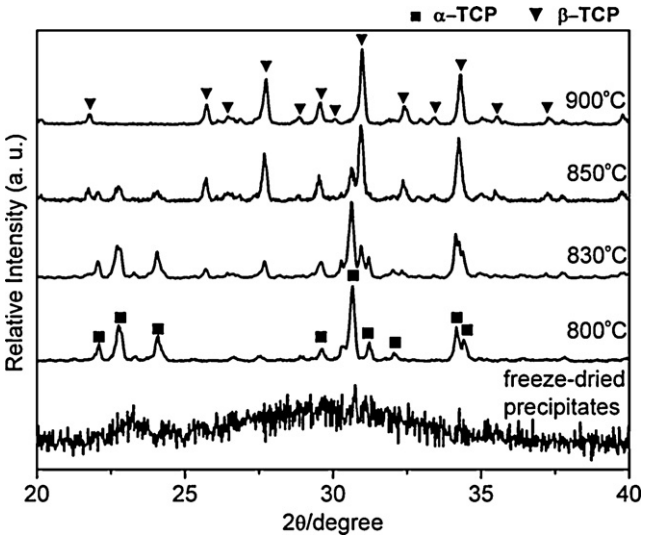

Fig. 2. XRD patterns of the freeze–dried precipitates and the calcined powders.

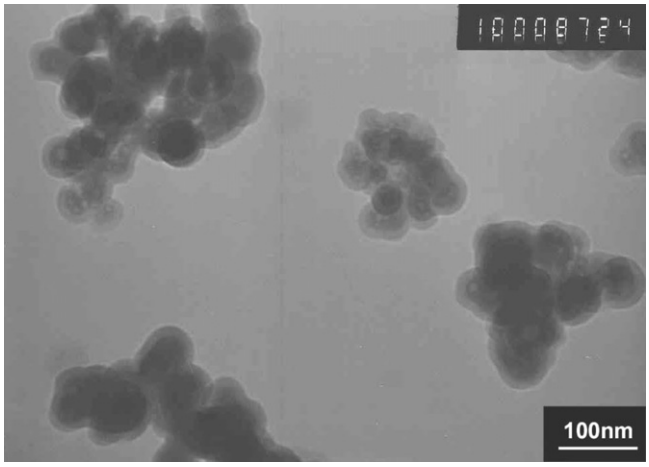

Fig. 3. TEM micrograph of freeze–dried precipitates.

Fig. 5. The sedimentation test results of the monophasic and biphasic TCPs.

BTCP60 and BTCP40 are used to represent the powders calcined at 830 °C and 850 °C, respectively.

The ACP precursor powders have a particle size of 40 nm (Fig. 3). Primary particles in the calcined powders still kept a spherical shape and have a size of about 500 nm, and the agglomerated particle size is about 1 μm, as shown in Fig. 4. The SAED patterns (Fig. 4) show that there exist two phases of α-TCP and β-TCP in one biphasic agglomerated particle. The sedimentation test (Fig. 5) shows that α-TCP and BTCP60 powders completely float in $C_2H_4Br_2$, while BTCP40 and β-TCP powders completely sedimentate in $C_2H_4Br_2$.

3.2. Behaviors of the TCP powders in acetate buffer solution

When the TCP powders are soaked in the acetate buffer solution with an initial pH 5, the pH value of the solution changes as the TCP powders react with the solution. The pH variation curves for different TCP powders are recorded as shown in Figs. 6 and 7.

These curves demonstrate that the pH value variation behavior depends on the α-TCP content in the TCP powders. The monophasic β-TCP powder shows to have one jump in pH from 5.0 to 5.32 after about 0.13 h soaking, then pH is kept unchanged (Fig. 6d), while the biphasic TCPs and monophasic α-TCP have two jumps in pH, pH in the first increase stage rises from 5.0 to 5.54 (0.12 h) for monophasic α-TCP, 5.51 (0.13 h) for BTCP60, and 5.50 (0.15 h) for BTCP40 (Fig. 6a–c). In the second increase stage, pH rises further

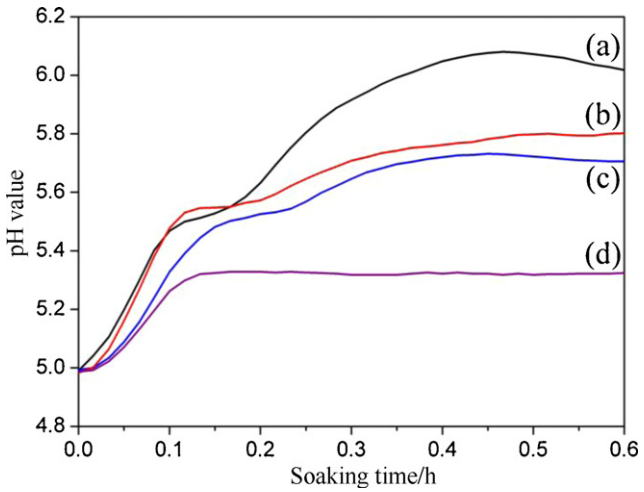

Fig. 6. pH curves of the monophasic and biphasic TCPs with soaking time during 0.6 h: (a) α-TCP, (b) BTCP60, (c) BTCP40, (d) β-TCP.

to 6.08(0.48 h) for monophasic α-TCP, 5.80(0.46 h) for BTCP60 and 5.73(0.43 h) for BTCP40 (Fig. 6a–c). The height of both the first and second jumps rises with increasing the α-TCP content in the TCP powders.

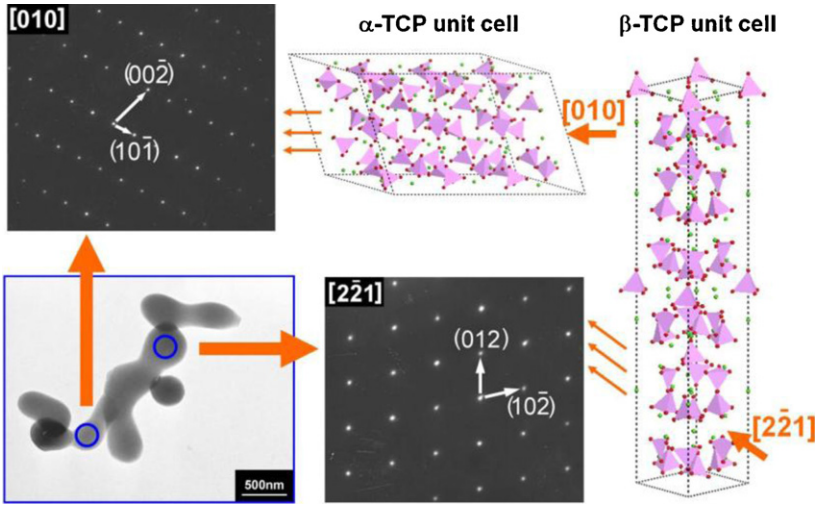

Fig. 4. TEM micrograph and SAED pattern of BTCP40 particle.

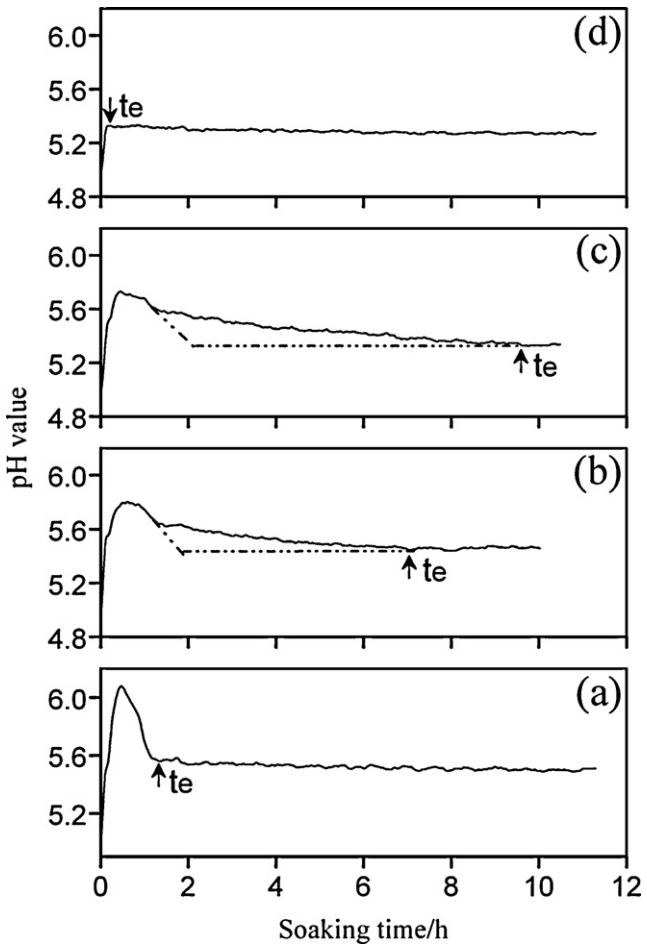

Fig. 7. pH curves of the monophasic and biphasic TCPs with soaking time during 12 h: (a) α-TCP, (b) BTCP60, (c) BTCP40, (d) β-TCP.

If the t_e is defined as the time for which the pH value begins to remain unchanged, monophasic TCPs have a small value of t_e, β-TCP is 0.13 h (just after the first jump), α-TCP is 1.5 h. However, biphasic TCPs have a large value of t_e, t_e is 6.6 h for BTCP40, and 9.5 h for BTCP60, respectively. The large t_e results in the formation of a peak shoulder (Fig. 7b and c) compared with α-TCP curve (Fig. 7a). It is noteworthy that the shoulder area in BTCT40 is larger than that in BTCP60.

After the powders are soaked in the acetate buffer solution, the XRD patterns of the resulting powders show a change in the crystalline phase (Fig. 8). For 0.5 h soaked TCPs: (i) the monophasic α-TCP powder is partially transformed to $CaHPO_4{\cdot}2H_2O$, (ii) all α-TCP in both biphasic TCPs is transformed to $CaHPO_4{\cdot}2H_2O$, (iii) no change takes place in the monophasic β-TCP powder. For 12 h soaked TCPs, after it is completely transformed into brushite, the monophasic α-TCP powder is converted to apatite. However, if brushite in the 0.5 h soaked BTCP60 powders is changed to apatite, it remains unchanged in the 0.5 h soaked BTCP40 powders. Notice that the monophasic β-TCP powders begin to transform to CaHPO4·2H2O.

The SEM micrographs of 12 h soaked TCPs demonstrate that: spherical shape of the particles changes to a cluster of petal-like crystallites for monophasic α-TCP powders (Fig. 9a); spherical particles are homogeneously distributed within clusters of petal-like crystallites for BTCP60 powders (Fig. 9b); petal-like crystallites are homogeneously distributed in spherical particles for BTCP40 powders (Fig. 9c); the particle shape has almost no change for monophasic β-TCP powders except that the connection between particles, which becomes thicker (Fig. 9d).

4. Discussion

4.1. Characteristics of the biphasic TCP

ACP consists of $Ca_9(PO_4)_6$ units close to those found in the apatite and TCP. The units are agglomerated into larger particles with water or polymeric molecules playing the role of a binder or stabilizer [39,40]. When the ACP is calcined with removal of the binders or stabilizers, the units tend to rearrange into an order structure through crystallization. The firstly crystallized phase from ACP at 800 °C is metastable α-TCP rather than stable β-TCP (Fig. 2), it is thought, for α-TCP, to form faster from the ACP than β-TCP [37]. An elevated calcination temperature will result in favorable kinetic conditions. Thus, the transformation of α-TCP to a more thermodynamically stable β-TCP is enhanced. Hence, the transformation degree of α-TCP to β-TCP increases with temperature under a fixed calcination time (3 h). The XRD data are consistent with this tendency (Fig. 2). As shown by the XRD data, the powder calcined at 830 °C and 850 °C is biphasic, and has 60 wt% and 40 wt% α-TCP, respectively, and is completely converted in β-TCP when it is calcined at 900 °C.

After calcination, the calcined powders still have a reasonably small primary and agglomerated particle size (Fig. 4). This is attributed to the ACP precursor particles with a much smaller particle size (40 nm) (Fig. 3) and the relatively low calcination temperature (800–900 °C). The SAED pattern (Fig. 4) proves that α-TCP and β-TCP primary particles coexist in the one biphasic

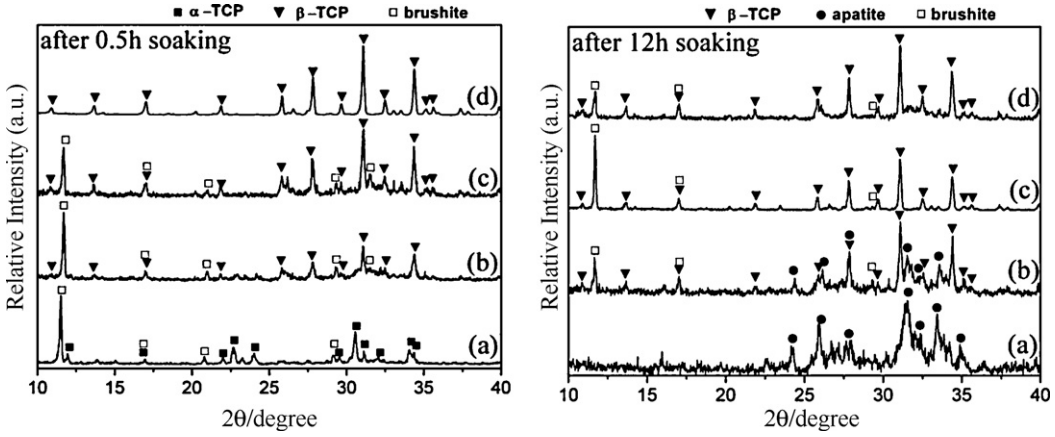

Fig. 8. XRD patterns of the TCPs after 0.5 h and 12 h soaked: (a) α-TCP, (b) BTCP60, (c) BTCP40, (d) β-TCP.

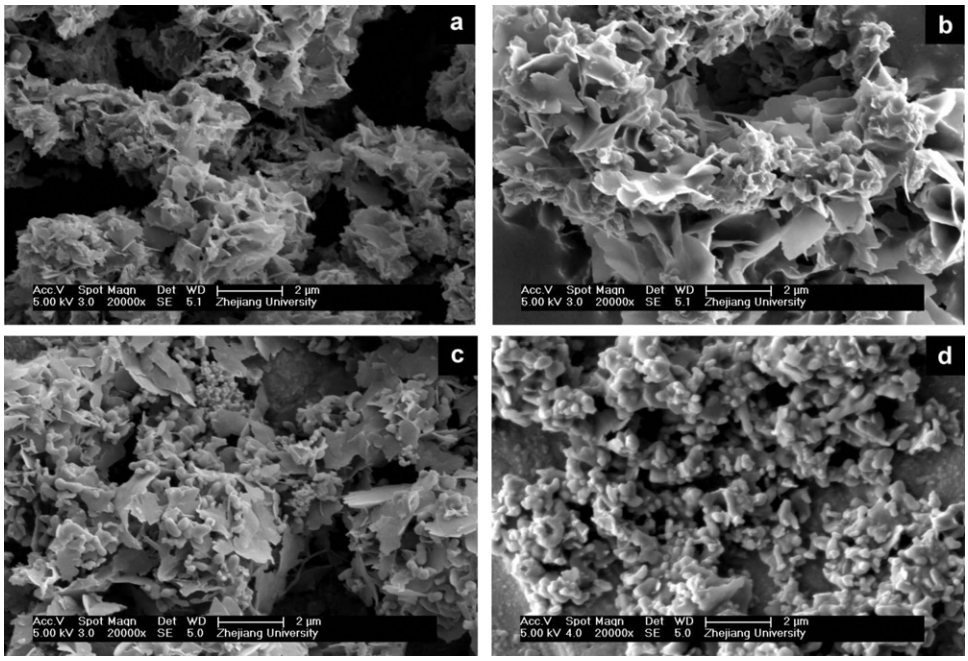

Fig. 9. SEM micrographs of the 12 h soaked TCP powders: (a) α-TCP, (b) BTCP60, (c) BTCP40, (d) β-TCP.

TCP agglomerated particle. And either a complete float or complete sedimentation of the biphasic powders in $C_2H_4Br_2$ (Fig. 5) strongly evidences that the two-phase particles are homogenously distributed in each agglomerated particle. The coexistence and homogenous distribution may result from the ACP precursor with the homogeneous size distributions of the primary and agglomerated particles.

Hence, the ACP derived biphasic TCP powders have small primary and agglomerated particle sizes. α-TCP and β-TCP primary particles not only coexist, but also are homogeneously distributed in each biphasic TCP agglomerated particle.

4.2. Dissolution–reprecipitation behavior of the biphasic TCP in acetate buffer solution

When the TCP powders are soaked in an acetate buffer solution with pH 5, the powders react with the solution as

$$Ca_3(PO_4)_2 \rightarrow 3Ca^{2+} + 2PO_4{}^{3-} \quad (1)$$

The appearance of phosphate ions changes the equilibrium between the acetic acid and acetate in the buffer solution. As a result, the pH value is raised with increasing the phosphate concentration as shown by Fig. 10. The pH variation curves (Figs. 6 and 7) of the TCP powders demonstrate to have two increase stages, one decrease stage and one plateau stage.

4.2.1. The first increase stage

For the first pH increase stage occurring at around 0.14 h as shown in Fig. 6, the pH value goes up to 5.32–5.54 depending on α-TCP content in the TCP powders. According to Fig. 10, as the pH value in the acetate buffer solution reaches 5.32 or 5.54, 0.85 mM [PO_4] or 4.36 mM [PO_4] should be present in the solution. These amounts are estimated to correspond to the dissolution of 1.32 or 6.76 wt%, respectively of the TCP powders, or of about 11 or 58 Å, respectively thickness surface layer of the 500 nm particles. Hence, it is suggested that the first pH increase stage may result from the dissolution of the TCP particle surface layer where the TCP has high dissolution ability because the atom arrangement structure is more disordered than that in the inner. The TCP powders with more α-TCP lead to a higher pH value, which could be attributed to the higher reactivity of α-TCP.

4.2.2. The second increase stage

When the dissolution of the TCP particle surface layer is completed, the inner TCP begins to react with the solution. Thus, the reaction (1) occurs more easily for α-TCP than β-TCP [7,10], causing a further increase in [PO_4], which is responsible for the second pH increase stage (Fig. 7). A higher content of α-TCP in the TCP powders leads to a much larger dissolved amount, resulting in a higher height of the second pH increase stage. No occurrence of the second increase stage in β-TCP powders indicates that the dissolution of β-TCP is too moderate to induce an obvious change in the pH value.

4.2.3. The decrease stage and the plateau stage

Ca and phosphate ion concentrations in solutions are impossible to increase unlimitedly because Ca phosphates have a very

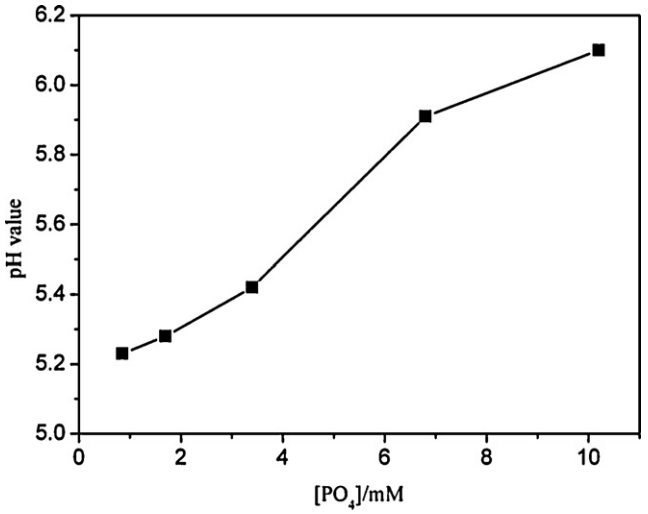

Fig. 10. A reference curve of phosphate concentration versus pH value in the acetate buffer solution with initial pH 5.

small solubility [37]. As a result, a reprecipitation takes place. Based on the initial acetate buffer solution with pH 5 and without any Ca^{2+} and PO_4^{3-} ions, the reprecipitation process during the initial soaking period (0.5 h) could be described as follows:

The phosphate ions from TCP dissolution are hydrolyzed in the acetate buffer solution:

$$H^+ + PO_4^{3-} \rightarrow HPO_4^{2-} \quad (2)$$

$$H^+ + HPO_4^{2-} \rightarrow H_2PO_4^- \quad (3)$$

$$H^+ + H_2PO_4^- \rightarrow H_3PO_4 \quad (4)$$

Then, Ca ions react with hydrogen phosphate to form $CaHPO_4{\cdot}2H_2O$ (brushite) (Fig. 8):

$$Ca^{2+} + HPO_4^{2-} + 2H_2O \rightarrow CaHPO_4{\cdot}2H_2O \quad (5)$$

Since the Ca/P ratio in dissolved ions from TCP is 1.5 and the Ca/P ratio in reprecipitated product is 1, the reprecipitation causes to exhaust more phosphate ions compared with Ca ions. As a result, the pH value decreases with proceeding of reaction (5). A fast dissolution of α-TCP leads to an extensive supersaturation, causing a high height of the second pH increase stage. Once crystalline nuclei form, the reprecipitation is accelerated under the extensive supersaturation, which causes the second pH increase stage to decrease rapidly.

Based on reaction (5), the amount of the reprecipitated product is closely related to the dissolution ability of the powders. This is quite in good agreement with the results of Fig. 8 in which the XRD intensity of brushite increases with α-TCP content in the TCP powders. The dissolution amount of β-TCP is too small to produce XRD detectable reprecipitation, and to have the second increase stage (Fig. 7d).

4.2.4. The differences in biphasic TCP

Monophasic α-TCP and β-TCP powders both have small t_e values. It is attributed to α-TCP with a fast dissolution–reprecipitation process, and β-TCP with no second pH increase stage due to a very slow dissolution–reprecipitation process, while the biphasic TCP powders have large t_e values, 6.6 and 9.5 h for BTCP60 and BTCP40, respectively. It is obvious that the dissolution–reprecipitation behavior of the biphasic TCP is not a simple combination of individual monophasic α-TCP and β-TCP contributions. Also this indicates that the mutual influence on the behavior from the two phases in the powders occurs.

As mentioned above, the α-TCP primary particles are surrounded by β-TCP primary particles in an agglomerated biphasic TCP particle. Thus, the hydrolysis (dissolution–reprecipitation) of α-TCP in the solution should be affected by neighboring β-TCP particles and surrounding extent, i.e. steric hindrance. The steric hindrance could be evidenced by their morphological changes (Fig. 9). The 12 h soaked biphasic TCP with more α-TCP (BTCP60) shows a small amount of spherical particles (undissolved β-TCP) distributed homogeneously within clusters of petal-like crystallites (hydrolyzed α-TCP) (Fig. 9b); Similarly, the 12 h soaked biphasic TCP with less α-TCP (BTCP40) is a small amount of petal-like crystallites distributed homogeneously within spherical particles (Fig. 9c). The integration of petal-like crystallites with spherical particles in the soaked biphasic powders undoubtedly results from the homogeneous distribution of α-TCP and β-TCP primary particles in each agglomerated particle.

Based on the above morphologic changes, the BTCP40 should have a more intensively steric hindrance for the α-TCP hydrolysis than the BTCP60. As a result, the BTCP40 has a relatively longer t_e than BTCP60 in pH curve (Fig. 7).

Hence, the present biphasic TCP powders demonstrate to be capable of tailoring TCP properties including the dissolution ability and morphological change through adjusting the two-phase ratio.

4.2.5. The changes in the precipitate after 12 h soaking

Reactions (1) and (5) proceed for a relatively long time, Ca ion concentration is increased. This makes the precipitated product have a higher Ca/P ratio than $CaHPO_4{\cdot}2H_2O$. Fig. 8a shows that the 12 h soaked α-TCP powders are totally transformed to apatite, the precipitate phase transformation reaction can be schematically written as:

$$6\{CaHPO_4{\cdot}2H_2O\} + (4-x)Ca^{2+} + (8-2x)OH^- \rightarrow Ca_{10-x}(HPO_4)_x(PO_4)_{6-x}(OH)_{2-x}\,(0 < x < 1) + (18-x)H_2O \quad (6)$$

The transformation also depends on the dissolution amount, the biphasic TCP powder with a high α-TCP content (BTCP60) can demonstrate a partial transformation (Fig. 8b), while that with a low α-TCP content (BTCP40) has no transformation (Fig. 8c). For β-TCP powders, reaction (1) prolongs for a long time to reach a critical concentration of Ca and phosphate ions, brushite precipitate eventually appears in the soaked powders (Fig. 8d).

5. Conclusions

The ACP derived biphasic TCP powders have a unique microstructural character of the coexistence and homogeneous distribution of 500 nm α-TCP and β-TCP primary particles in each 1 μm agglomerated particle. The assembly of nano-sized particles with different phases into one small agglomeration could be an effective microstructural organization way to modulate material properties for creating desired performances. The strong dependence of the dissolution–reprecipitation behavior of the biphasic TCPs on α-TCP/β-TCP ratio is attributed to the α-TCP hydrolysis, which is significantly retarded by the presence of β-TCP due to steric hindrance. Hence, the biphasic TCP powders could play an important role in the TCP related biomaterials for bone repair and reconstruction.

Acknowledgements

The authors would like to thank Ruibin Wang, Lili Pan and Huibin Liu for the sample preparation and pH measurement.

References

[1] K. de Groot, C.P.A.T. Klein, J.G.C. Wolke, J.M.A. de Blieck-Hogervorst, Handbook of Bioactive Ceramics, in: T. Yamamuro, L. Hench, J. Wilson (Eds.), Chemistry of Calcium Phosphate Bioceramics, CRC Press, Boston, 1990, pp. 3–16.
[2] E. Kawachi, C. Bertran, L. Kubota, Biomaterials 19 (1998) 2329–2333.
[3] J. Huang, L. Zhang, B. Chu, X. Peng, S. Tang, Artif. Organs 35 (2011) 49–57.
[4] R. Rohanizadeh, M. Padrines, J. Bouler, D. Couchourel, Y. Fortun, G. Daculsi, J. Biomed. Mater. Res. A 42 (1998) 530–539.
[5] W. Min, K. Daimon, Y. Doi, T. Suzuki, Y. Hikichi, M. Miyamoto, J. Alloys Compd. 311 (2000) 79–81.
[6] Y. Li, X. Zhang, K.D. Groot, Biomaterials 18 (1997) 737–741.
[7] F. Lin, C. Liao, K. Chen, J. Sun, C. Lin, Biomaterials 22 (2001) 2981–2992.
[8] M. Neo, H. Herbst, C.F. Voigt, U.M. Gross, J. Biomed. Mater. Res. 39 (1998) 71–76.
[9] E. Verron, I. Khairoun, J. Guicheux, J. Bouler, Drug Discov. Today 15 (2010) 547–552.
[10] L. Hench, J. Am. Ceram. Soc. 81 (1998) 1705–1728.
[11] S. Dorozhkin, M. Epple, Angew. Chem. Int. Ed. 41 (2002) 3130–3146.
[12] Z. Seeley, A. Bandyopadhyay, S. Bose, Mater. Sci. Eng. C 28 (2008) 11–17.
[13] L. Pan, Y. Li, W. Weng, K. Cheng, C. Song, P. Du, G. Zhao, G. Shen, J. Wang, G. Han, Key Eng. Mater. 309 (2006) 219–222.
[14] H. Hu, X. Liu, C. Ding, J. Alloys Compd. 498 (2010) 172–178.
[15] I. Manjubala, T. Sastry, R. Kumar, J. Biomater. Appl. 19 (2005) 341.
[16] S. Li, J. de Wijn, J. Li, P. Layrolle, K. de Groot, Tissue Eng. 9 (2003) 535–548.
[17] M. Alam, I. Asahina, K. Ohmamiuda, S. Enomoto, J. Biomed. Mater. Res. 54 (2001) 129–138.

[18] S.S. Banerjee, A. Bandyopadhyay, S. Bose, Adv. Eng. Mater. 12 (2010) B148–B155.
[19] M. Zheng, D. Fan, X. Li, J. Zhang, Q. Liu, J. Alloys Compd. 489 (2010) 211–214.
[20] J.S. Cho, Y.C. Kang, J. Alloys Compd. 464 (2008) 282–287.
[21] G. Chen, W. Li, B. Zhao, K. Sun, J. Am. Ceram. Soc. 92 (2009) 945–948.
[22] M. Kamitakahara, C. Ohtsuki, M. Oishi, S. Ogata, T. Miyazaki, M. Tanihara, Key Eng. Mater. 284 (2005) 281–284.
[23] S. Sanchez-Salcedo, F. Balas, I. Izquierdo-Barba, M. Vallet-Regi, Acta Biomater. 5 (2009) 2738–2751.
[24] K. Flade, C. Lau, M. Mertig, W. Pompe, Chem. Mater. 13 (2001) 3596–3602.
[25] H. Zeng, K. Chittur, W. Lacefield, Biomaterials 20 (1999) 443–451.
[26] Y. Li, D. Li, W. Weng, Key Eng. Mater. 368 (2008) 1206–1208.
[27] B. Boonchom, J. Alloys Compd. 482 (2009) 199–202.
[28] W.J. Shih, S.H. Wang, W.L. Li, M.H. Hon, M.C. Wang, J. Alloys Compd. 434–435 (2007) 693–696.
[29] W.A. Badawy, A.M. Fathi, R.M. El-Sherief, S.A. Fadl-Allah, J. Alloys Compd. 475 (2009) 911–916.
[30] S.L. Zhu, X.J. Yang, Z.D. Cui, J. Alloys Compd. 504 (2010) S168–S171.
[31] A. Feng, Y. Han, J. Alloys Compd. 504 (2010) 585–593.
[32] Y. Doi, T. Shibutani, Y. Moriwaki, T. Kajimoto, Y. Iwayama, J. Biomed. Mater. Res. A 39 (1998) 603–610.
[33] M.H. Fathi, E.M. Zahrani, J. Alloys Compd. 475 (2009) 408–414.
[34] G. Daculsi, O. Laboux, O. Malard, P. Weiss, J. Mater. Sci. Mater. Med. 14 (2003) 195–200.
[35] J.C. Elliot, Structure and Chemistry of the Apatites and Other Calcium Orthophosphates, Elsevier Science, Amsterdam, 1994.
[36] J. Ando, Bull. Chem. Soc. Jpn. 31 (1958) 196–201.
[37] T. Kanazawa, Inorganic Phosphate Materials, Elsevier Science, Tokyo, 1989.
[38] Y. Li, W. Weng, K. Tam, Acta Biomater. 3 (2007) 251–254.
[39] Y. Li, W. Weng, K. Cheng, P. Du, G. Shen, J. Wang, G. Han, J. Mater. Sci. Lett. 22 (2003) 1015–1016.
[40] Y. Li, W. Weng, K. Cheng, P. Du, G. Shen, G. Han, Mater. Sci. Technol. 20 (2004) 1075–1078.